International Journal of Innovative Computing, Information and Control
Volume **21**, Number **2**, April **2025**

ICIC International ©2025 ISSN 1349-4198
pp. **407–422**

OPTIMAL SURFACE IN PLAN FOR HOLLOW CIRCULAR FOOTINGS ASSUMING THAT THE CONTACT SURFACE WITH SOIL WORKS PARTIALLY UNDER COMPRESSION

Eyran Roberto Diaz-Gurrola[1], Arnulfo Luévanos-Rojas[1,*]
Gloria Josefina Montiel-Sánchez[2] and Carmela Martínez-Aguilar[1]

[1]Instituto de Investigaciones Multidisciplinaria
Facultad de Contaduría y Administración
Universidad Autónoma de Coahuila, Unidad Torreón
Blvd. Revolución 151 Ote. CP 27000, Torreón, Coahuila, México
{ eyran_diaz; carmelamartinez }@uadec.edu.mx
*Corresponding author: arnulfoluevanos@uadec.edu.mx

[2]Centro de Estudios Tecnológicos Industriales y de Servicios No. 59
Calle Mayela S/N Col. Ampliación Margaritas. CP 27130, Torreón, Coahuila, México
gloria.montiel.ce59@dgeti.sems.gob.mx

Received August 2024; revised November 2024

Abstract. *This paper presents a model to determine the optimal surface of a hollow circular footing or annular strip footing (the width and the position where pressure is zero, since the radius is subject to the conditions of the superstructure), assuming that the soil is elastic, the soil pressure distribution is linear and the surface in contact with the soil works partially in compression. Some authors show the optimal surface of solid circular footings taking it into account that the area in contact with the soil works partially under compression, and other present annular strip footings or hollow circular footings assuming uniform soil pressure. The formulation is developed by integration to determine the axial load "P" and a resultant moment "M_R" from the moments "M_x" and "M_y". Six numerical examples are presented to determine the soil contact area for hollow circular footings under an axial load and a resultant moment. A comparison is also made with the results of other authors and the results show that using the proposed model savings of up to 43.75% can be achieved.*

Keywords: Optimal surface, Hollow circular footings, Linear soil pressure, Partially compressed contact surface

1. **Introduction.** A circular footing is a shallow foundation used to support the structures with circular geometry such as water tanks, wind turbines, and silos. A ring footing is a shallow foundation, also called as annular footing, used to support isolated structures with annular geometry such as lighthouses, chimneys, and silos. A strip footing, also called as continuous footing is a shallow foundation used to support long structures having load-bearing walls.

Some researchers have developed models to determine the plan contact surface for various types of solid foundations: Isolated square, rectangular and circular footings subjected to biaxial bending [1-10]; Combined trapezoidal, rectangular, strap and T-shaped footings subjected to biaxial bending in each column [11-15]. All these models assume that the contact surface in plan works entirely in compression.

Several researchers have investigated complete models to determine the footings design for various types of solid foundations: Isolated square, rectangular and circular footings

DOI: 10.24507/ijicic.21.02.407

subjected to biaxial bending [16-20]; Combined trapezoidal, rectangular, strap and T-shaped footings subjected to biaxial bending in each column [21-26]. All these models assume that the contact surface in plan works entirely in compression.

Other researchers have proposed models to determine the plan contact surface for various types of solid footings assuming that soil contact surface works partially to compression and a linear soil pressure distribution: Isolated footings subjected to biaxial bending for rectangular [27-36] and circular shapes [37-39]; Rectangular combined footings subjected to biaxial bending in each column [40].

Several researchers have studied to determine the complete footings design for various types of solid foundations assuming that soil contact surface works partially to compression and a linear soil pressure distribution: Isolated footings subjected to biaxial bending for rectangular [41] and circular shapes [42].

The works on hollow circular footings or annular footings are as follows. Singh-Rathor et al. [43] investigated an annular foundation supported by reinforced concrete piles based on the continuum approach. Kim et al. [44] applied the finite element method to obtaining the bearing capacity of an annular foundation resting on medium to highly weathered rocks. Sankaran and Subrahmanyam [45] presented analytical solutions the contact pressure distribution for uniform load in annular ring showing curves and numerical examples. Rathor and Sharma [46] developed a comparison between solid raft foundations and annular raft foundations. Galvis and Smith-Pardo [47] estimated simplified closed-form equations and design aids to obtain the coupled vertical load and biaxial moment capacity for hollow and solid circular and rectangular shallow foundations. Ahmad et al. [48] presented an analysis of ring footings and anchors supported on elastic soil medium using finite difference technique. Rana and Jamani [49] showed a comparison between solid circular raft foundations and annular raft circular foundations for water tank with different diameters. Kumar and Rai [50] presented a comparative analysis of ring slab foundations with ring beam and without ring beam. Manideep et al. [51] evaluated the bearing capacity of circular, ring and footings on limited depth of soil.

According to the bibliographic review, there are several studies on rectangular and circular isolated footings assuming that the area in contact with the ground works partially under compression (solid footings without gaps), on the other hand there are also several works on annular foundations or hollow circular footings assuming uniform soil pressure, that is, this pressure is the bearing capacity of the soil. Therefore, there is no paper on optimal surface in plan for hollow circular footings assuming that the contact surface with soil works partially to compression.

This paper presents a model to estimate the optimal surface of a hollow circular footing or annular strip footing assuming that contact surface with the ground works partially in compression, that is, one part of the contact surface of the footing with ground is subjected to compression and the other part has zero pressure (The width is defined, since the radius is subject to the conditions of the superstructure). Some authors show the optimal surface of a solid circular footing, and others present annular strip footings or hollow circular footings assuming uniform soil pressure. Six numerical examples are shown to estimate the contact surface of hollow circular footings under an axial load and a resultant moment, and a comparison is also made with other authors to observe the differences.

The paper is organized as follows. Section 2 describes the formulation of the model to determine the dimension of the hollow circular footings assuming that contact surface with the ground works partially to compression. Subsection 2.1 shows the equations for case I (Surface works entirely in compression). Subsection 2.2 presents the equations for case II (Surface works partially in compression). Subsection 2.3 shows the optimal surface

for hollow circular footings of the two cases. Section 3 presents the numerical examples applied to the new model for hollow circular footings. Section 4 shows the results. Section 5 presents the conclusions to complete the paper.

2. **Formulation of the Model.** Figure 1 presents a hollow circular footing under biaxial bending.

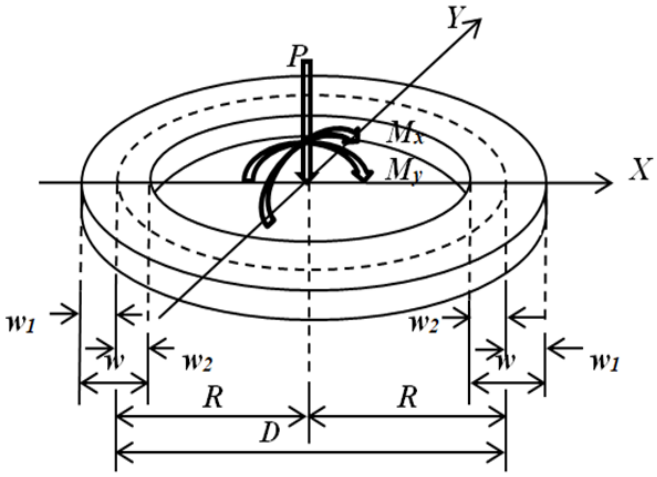

FIGURE 1. Hollow circular footing for two moments

General equation of the biaxial bending for footings is

$$p_s = \frac{P}{A} + \frac{M_x y}{I_x} + \frac{M_y x}{I_y} \tag{1}$$

where p_s = soil pressure on the base, A = contact area in plan of the footing, P = axial load applied to the footing, M_x and M_y = moments applied on their respective axes, x and y = coordinates of the footing under study, I_x and I_y = moments of inertia on their respective axes.

Now, to work the problem with a moment, the resultant moment "M_R" is determined from the two moments "M_x" and "M_y".

Figure 2 shows the axial load "P" and the resultant moment "M_R" of the moments applied to the X and Y axes, the width of the foundation "w", the external width of the foundation "w_1", the internal width of the foundation "w_2", the radius of the wall "R" and the diameter of the wall "D".

The resultant moment "M_R" is obtained as shown below:

$$M_R = \sqrt{{M_x}^2 + {M_y}^2} \tag{2}$$

The inclination angle "φ" is obtained from the Y axis as shown below:

$$\sin\varphi = \frac{M_y}{M_R} \rightarrow \varphi = \arcsin\left(\frac{M_y}{M_R}\right) \tag{3}$$

Substituting Equation (2) into Equation (1) is obtained the soil pressure on the hollow circular footing as shown below:

$$p_s = \frac{P}{A} + \frac{M_R y_R}{I} \tag{4}$$

where y_R = coordinate of the footing on the Y' axis.

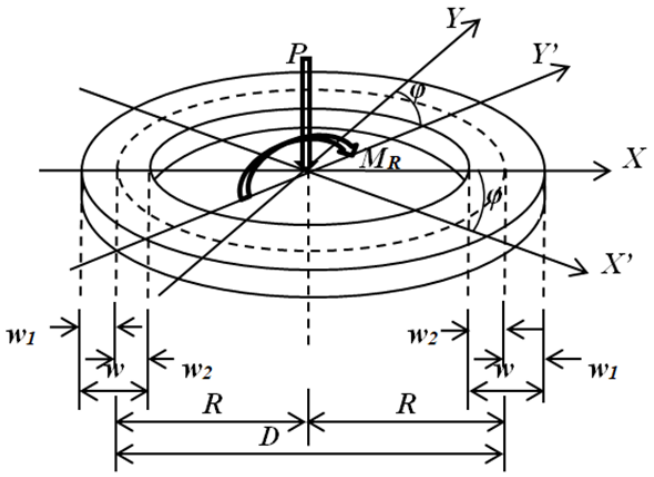

FIGURE 2. Simplified hollow circular footing

Substituting $A = \pi(R + w_1)^2 - \pi(R - w_2)^2$ and $I = \pi(R + w_1)^4/4 - \pi(R - w_2)^4/4$ into Equation (4), the maximum pressure "p_{s1}" and minimum pressure "p_{s2}" of the hollow circular footing are determined:

$$p_{s1} = \frac{P}{\pi\left[(R + w_1)^2 - (R - w_2)^2\right]} + \frac{4M_R\,(R + w_1)}{\pi\left[(R + w_1)^4 - (R - w_2)^4\right]} \tag{5}$$

$$p_{s2} = \frac{P}{\pi\left[(R + w_1)^2 - (R - w_2)^2\right]} - \frac{4M_R\,(R + w_1)}{\pi\left[(R + w_1)^4 - (R - w_2)^4\right]} \tag{6}$$

where w_1 = outside width of the foundation measured from the center of the wall, w_2 = inside width of the foundation measured from the center of the wall.

The eccentricity equation "e_R" is obtained as shown below:

$$e_R = \frac{M_R}{P} \tag{7}$$

Figure 3 presents a circular footing. In this type of foundations, two cases appear: Case I when the resultant force is located inside the central nucleus, that is, the entire area works in compression; Case II when the resultant force is located outside the central nucleus, that is, a part of the area works in compression (well-known situation).

Figure 4 presents the pressure diagram of a hollow circular footing for the two cases.

2.1. **Case I. Surface works entirely in compression.** Figure 4(a) presents the pressure diagram of a hollow circular footing supported on elastic soils with an eccentric column under biaxial bending; assuming that the surface in contact with the ground works completely in compression and the distribution of the ground pressure is linear.

General equations for a hollow circular footing are shown in Equations (5) and (6).

2.2. **Case II. Surface works partially in compression.** Figure 4(b) presents the pressure diagram of a hollow circular footing supported on elastic soils with an eccentric column under biaxial bending; assuming that the surface in contact with the ground works partially in compression and the distribution of the ground pressure is linear.

The relationship between the pressure at anywhere of the footing "p_z" and the maximum pressure "$p_{\max}$" is found as follows:

$$\frac{p_z}{y' - y_0} = \frac{p_{\max}}{R + w_1 - y_0} \tag{8}$$

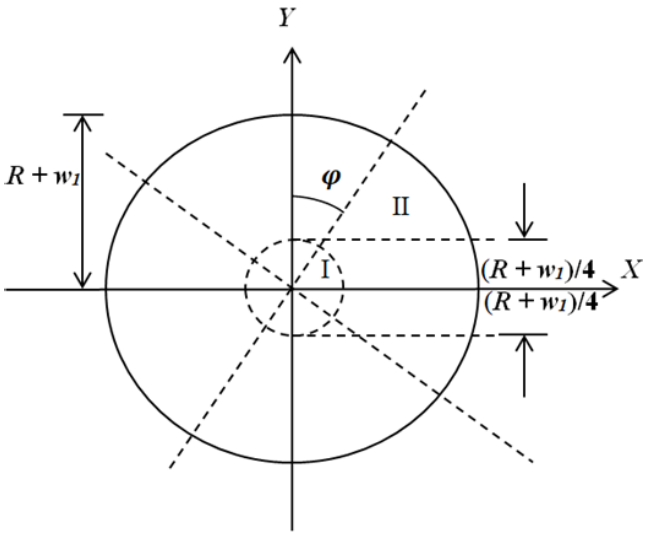

FIGURE 3. Central nucleus of a circular footing

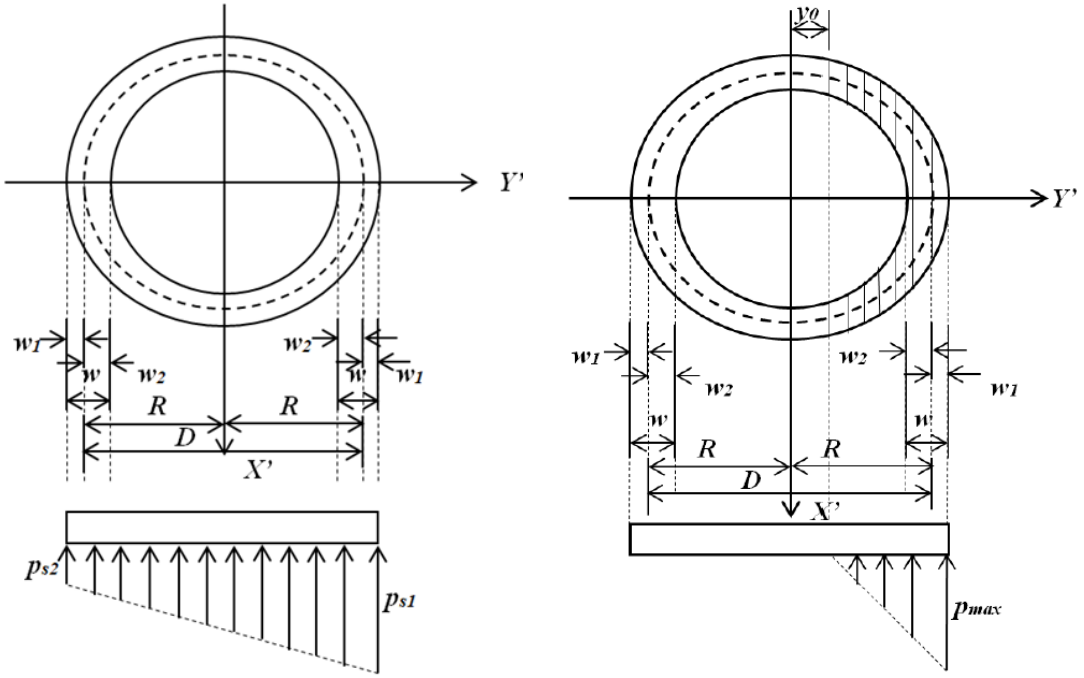

(a) Case I (b) Case II

FIGURE 4. Pressure diagram of a hollow circular footing

By Equation (8), the pressure at anywhere of the hollow circular footing is determined:

$$p_z = \frac{p_{\max}\,(y' - y_0)}{R + w_1 - y_0} \tag{9}$$

To obtain the vertical load, it is done in two parts, the first for the circumference of radius $R + w_1$, and the second for the circumference of radius $R - w_2$.

Now, by integration the vertical load generated by the soil pressure is obtained.

For the circumference of radius $R + w_1$:

$$P_1 = \int_{y_0}^{R+w_1} p_z dA \tag{10}$$

where

$$dA = 2x'dy' \tag{11}$$

$$x' = \sqrt{(R + w_1)^2 - y'^2} \tag{12}$$

Substituting Equations (9), (11) and (12) into Equation (10) is obtained:

$$P_1 = 2\int_{y_0}^{R+w_1} \frac{p_{\max}(y' - y_0)}{R + w_1 - y_0}\sqrt{(R + w_1)^2 - y'^2}dy' \tag{13}$$

$$P_1 = \frac{p_{\max}}{R + w_1 - y_0}\left\{\frac{\left[2(R + w_1)^2 + {y_0}^2\right]\sqrt{(R + w_1)^2 - {y_0}^2}}{3}\right.$$

$$\left. - \frac{y_0(R + w_1)^2}{2}\left[\pi - 2\arcsin\left(\frac{y_0}{R + w_1}\right)\right]\right\} \tag{14}$$

For the circumference of radius $R - w_2$:

$$P_2 = \int_{y_0}^{R-w_2} p_z dA \tag{15}$$

where

$$dA = 2x'dy' \tag{16}$$

$$x' = \sqrt{(R - w_2)^2 - y'^2} \tag{17}$$

Substituting Equations (9), (16) and (17) into Equation (15) is obtained:

$$P_2 = 2\int_{y_0}^{R-w_2} \frac{p_{\max}(y' - y_0)}{R + w_1 - y_0}\sqrt{(R - w_2)^2 - y'^2}dy' \tag{18}$$

$$P_2 = \frac{p_{\max}}{R + w_1 - y_0}\left\{\frac{\left[2(R - w_2)^2 + {y_0}^2\right]\sqrt{(R - w_2)^2 - {y_0}^2}}{3}\right.$$

$$\left. - \frac{y_0(R - w_2)^2}{2}\left[\pi - 2\arcsin\left(\frac{y_0}{R - w_2}\right)\right]\right\} \tag{19}$$

Now, the total load "P" is obtained from $P_1 - P_2$.

$$P = \frac{p_{\max}}{R + w_1 - y_0}\left\{\frac{\left[2(R + w_1)^2 + {y_0}^2\right]\sqrt{(R + w_1)^2 - {y_0}^2}}{3}\right.$$

$$- \frac{\left[2(R - w_2)^2 + {y_0}^2\right]\sqrt{(R - w_2)^2 - {y_0}^2}}{3}$$

$$- \frac{y_0(R + w_1)^2}{2}\left[\pi - 2\arcsin\left(\frac{y_0}{R + w_1}\right)\right]$$

$$\left. + \frac{y_0(R - w_2)^2}{2}\left[\pi - 2\arcsin\left(\frac{y_0}{R - w_2}\right)\right]\right\} \tag{20}$$

Now, by integration the resultant moment generated by the soil pressure is obtained.

For the circumference of radius $R + w_1$:

$$M_{R1} = \int_{y_0}^{R+w_1} p_z y' dA \tag{21}$$

Substituting Equations (9), (11) and (12) into Equation (21) is obtained:

$$M_{R1} = 2\int_{y_0}^{R+w_1} \frac{p_{\max}\left(y' - y_0\right)}{R + w_1 - y_0}\sqrt{\left(R + w_1\right)^2 - y'^2}\, y' dy' \tag{22}$$

$$M_{R1} = \frac{p_{\max}}{R + w_1 - y_0}\left\{\frac{y_0\left[5\left(R + w_1\right)^2 - 2{y_0}^2\right]\sqrt{\left(R + w_1\right)^2 - {y_0}^2}}{12}\right.$$

$$\left. - \frac{\left(R + w_1\right)^4}{8}\left[\pi - 2\arcsin\left(\frac{y_0}{R + w_1}\right)\right]\right\} \tag{23}$$

For the circumference of radius $R - w_2$:

$$M_{R2} = \int_{y_0}^{R-w_2} p_z y' dA \tag{24}$$

Substituting Equations (9), (16) and (17) into Equation (24) is obtained:

$$M_{R2} = 2\int_{y_0}^{R-w_2} \frac{p_{\max}\left(y' - y_0\right)}{R + w_1 - y_0}\sqrt{\left(R - w_2\right)^2 - y'^2}\, y' dy' \tag{25}$$

$$M_{R2} = \frac{p_{\max}}{R + w_1 - y_0}\left\{\frac{y_0\left[5\left(R - w_2\right)^2 - 2{y_0}^2\right]\sqrt{\left(R - w_2\right)^2 - {y_0}^2}}{12}\right.$$

$$\left. - \frac{\left(R - w_2\right)^4}{8}\left[\pi - 2\arcsin\left(\frac{y_0}{R - w_2}\right)\right]\right\} \tag{26}$$

Now, the total resultant moment "M_R" is obtained from $M_{R1} - M_{R2}$.

$$M_R = \frac{p_{\max}}{R + w_1 - y_0}\left\{\frac{y_0\left[5\left(R + w_1\right)^2 - 2{y_0}^2\right]\sqrt{\left(R + w_1\right)^2 - {y_0}^2}}{12}\right.$$

$$- \frac{y_0\left[5\left(R - w_2\right)^2 - 2{y_0}^2\right]\sqrt{\left(R - w_2\right)^2 - {y_0}^2}}{12}$$

$$- \frac{\left(R + w_1\right)^4}{8}\left[\pi - 2\arcsin\left(\frac{y_0}{R + w_1}\right)\right]$$

$$\left. + \frac{\left(R - w_2\right)^4}{8}\left[\pi - 2\arcsin\left(\frac{y_0}{R - w_2}\right)\right]\right\} \tag{27}$$

2.3. **Optimal surface for hollow circular footings.** The objective function to obtain the minimum area "$A_{\min}$" for the two cases is

$$A_{\min} = \pi\left[\left(R + w_1\right)^2 - \left(R - w_2\right)^2\right] \tag{28}$$

The constraint functions for axial load and moment for the two cases are presented in Table 1.

TABLE 1. Constraint functions for axial load and moment

Case	Constraint functions
I	Equations (5) and (6), $w = w_1 + w_2$, $R \geq w_2$, $w_1 \geq 1$, $w_2 \geq 1$, $p_{s1} \leq p_{\max}$, $0 \leq p_{s1}$, $p_{s2} \leq p_{\max}$, $0 \leq p_{s2}$
II	Equations (20) and (27), $w = w_1 + w_2$, $R \geq w_2$, $w_1 \geq 1$, $w_2 \geq 1$, $R \geq \lvert y_0 \rvert$

Figure 5 shows the flowchart using the equations proposed and how to use Maple software to determine the minimum area of a hollow circular footing (Nonlinear optimization).

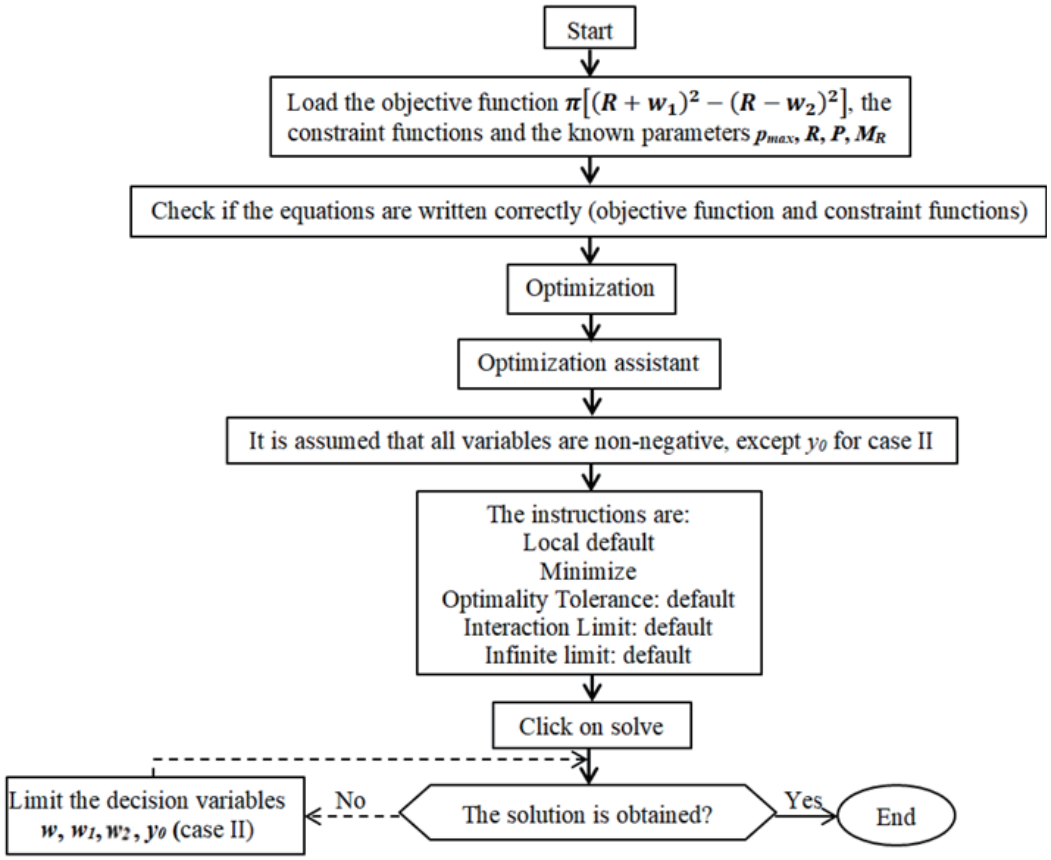

FIGURE 5. Flowchart for using Maple software

3. **Numerical Problems.** Tables 2, 3, 4, 5, 6 and 7 present six types of examples to obtain the dimensions of a hollow circular base. Type 1: The constant conditions are $P = 20000$ kN, $M_R = 350000$ kN-m, $R = 20.00$ m (w_1 and w_2 different), and changing "$p_{\max}$" (see Table 2). Type 2: The conditions are the same as type 1 (w_1 and w_2 equal) (see Table 3). Type 3: The constant conditions are $p_{\max} = 300$ kN/m^2, $M_R = 250000$ kN-m, $R = 15.00$ m (w_1 and w_2 different), and changing "P" (see Table 4). Type 4: The conditions are the same as type 3 (w_1 and w_2 equal) (see Table 5). Type 5: The constant conditions are $p_{\max} = 300$ kN/m^2, $P = 28000$ kN, $R = 15.00$ m (w_1 and w_2 different), and changing "M_R" (see Table 6). Type 6: The conditions are the same as type 5 (w_1 and w_2 equal) (see Table 7).

This procedure is used as follows:

1.- It starts with the data known as $p_{\max}$, R, P and M_R.

2.- The objective function is obtained by Equation (28).

3.- The constraint functions for each case are shown in Table 1.

4.- Once the objective function and the constraint functions are known, the procedure shown in Figure 5 is used to obtain the solution to the examples for case I ($A_{\min}$, w_1, w_2, w, p_1 and p_2), and for case II ($A_{\min}$, w_1, w_2, w and y_0).

TABLE 2. $P = 20000$ kN, $M_R = 350000$ kN-m, $R = 20.00$ m (w_1 and w_2 different)

Case	$p_{\max}$ kN/m^2	y_0 m	w_1 m	w_2 m	w m	p_1 kN/m^2	p_2 kN/m^2	$A_{\min}$ m^2
I	100	–	44.39	1.00	45.39	3.36	0	11892.72
II		1.25	4.37	1.00	5.37	100.00	0	730.99
I	150	–	44.39	1.00	45.39	3.36	0	11892.72
II		3.94	2.97	1.00	3.97	150.00	0	523.40
I	200	–	44.39	1.00	45.39	3.36	0	11892.72
II		5.48	2.18	1.00	3.18	200.00	0	411.28
I	250	–	44.39	1.00	45.39	3.36	0	11892.72
II		6.49	1.66	1.00	2.66	250.00	0	340.18
I	300	–	44.39	1.00	45.39	3.36	0	11892.72
II		7.21	1.30	1.00	2.30	300.00	0	290.71

TABLE 3. $P = 20000$ kN, $M_R = 350000$ kN-m, $R = 20.00$ m (w_1 and w_2 equal)

Case	$p_{\max}$ kN/m^2	y_0 m	w_1 m	w_2 m	w m	p_1 kN/m^2	p_2 kN/m^2	$A_{\min}$ m^2
I	100	–	–	–	–	–	–	–
II		5.80	3.75	3.75	7.50	100.00	0	942.15
I	150	–	–	–	–	–	–	–
II		6.93	2.49	2.49	4.98	150.00	0	624.86
I	200	–	–	–	–	–	–	–
II		7.39	1.84	1.84	3.68	200.00	0	461.61
I	250	–	–	–	–	–	–	–
II		7.60	1.45	1.45	2.90	250.00	0	364.13
I	300	–	–	–	–	–	–	–
II		7.72	1.19	1.19	2.38	300.00	0	299.96

TABLE 4. $p_{\max} = 300$ kN/m^2, $M_R = 250000$ kN-m, $R = 15.00$ m (w_1 and w_2 different)

Case	P kN	y_0 m	w_1 m	w_2 m	w m	p_1 kN/m^2	p_2 kN/m^2	$A_{\min}$ m^2
I	28000	–	13.94	1.00	14.94	27.78	0	2015.80
II		−11.38	1.27	1.00	2.27	300.00	0	215.79
I	26000	–	17.41	1.00	18.41	19.37	0	2685.21
II		−9.04	1.25	1.00	2.25	300.00	0	214.25
I	24000	–	21.26	1.00	22.26	13.66	0	3515.11
II		−6.12	1.27	1.00	2.27	300.00	0	216.18
I	22000	–	25.63	1.00	26.63	9.63	0	4570.53
II		−2.51	1.35	1.00	2.35	300.00	0	224.48
I	20000	–	30.71	1.00	31.71	6.72	0	5948.97
II		1.88	1.57	1.00	2.57	300.00	0	246.46

TABLE 5. $p_{\max} = 300$ kN/m^2, $M_R = 250000$ kN-m, $R = 15.00$ m (w_1 and w_2 equal)

Case	P kN	y_0 m	w_1 m	w_2 m	w m	p_1 kN/m^2	p_2 kN/m^2	$A_{\min}$ m^2
I	28000	–	–	–	–	–	–	–
II		−11.03	1.15	1.15	2.30	300.00	0	217.59
I	26000	–	–	–	–	–	–	–
II		−8.68	1.15	1.15	2.30	300.00	0	217.59
I	24000	–	–	–	–	–	–	–
II		−5.71	1.16	1.16	2.32	300.00	0	218.98
I	22000	–	–	–	–	–	–	–
II		−1.96	1.22	1.22	2.44	300.00	0	229.63
I	20000	–	–	–	–	–	–	–
II		2.79	1.38	1.38	2.76	300.00	0	260.77

TABLE 6. $p_{\max} = 300$ kN/m^2, $P = 28000$ kN, $R = 15.00$ m (w_1 and w_2 different)

Case	M_R kN-m	y_0 m	w_1 m	w_2 m	w m	p_1 kN/m^2	p_2 kN/m^2	$A_{\min}$ m^2
I	240000	–	12.04	1.00	13.04	33.32	0	1680.61
II		−12.41	1.20	1.00	2.20	300.00	0	209.21
I	260000	–	15.77	1.00	16.77	23.73	0	2359.42
II		−10.30	1.34	1.00	2.34	300.00	0	222.94
I	280000	–	19.28	1.00	20.28	18.20	0	3076.61
II		−8.03	1.50	1.00	2.50	300.00	0	239.22
I	300000	–	22.65	1.00	23.65	14.59	0	3837.88
II		−5.65	1.68	1.00	2.68	300.00	0	258.73
I	320000	–	25.93	1.00	26.93	12.05	0	4645.97
II		−3.22	1.91	1.00	2.91	300.00	0	282.47

TABLE 7. $p_{\max} = 300$ kN/m^2, $P = 28000$ kN, $R = 15.00$ m (w_1 and w_2 equal)

Case	M_R kN-m	y_0 m	w_1 m	w_2 m	w m	p_1 kN/m^2	p_2 kN/m^2	$A_{\min}$ m^2
I	240000	–	–	–	–	–	–	–
II		−12.16	1.12	1.12	2.24	300.00	0	210.41
I	260000	–	–	–	–	–	–	–
II		−9.84	1.20	1.20	2.40	300.00	0	225.52
I	280000	–	–	–	–	–	–	–
II		−7.32	1.30	1.30	2.60	300.00	0	244.19
I	300000	–	–	–	–	–	–	–
II		−4.63	1.42	1.42	2.84	300.00	0	267.92
I	320000	–	–	–	–	–	–	–
II		−1.83	1.59	1.59	3.18	300.00	0	299.37

4. **Results.** Table 2 presents the following. Case I: All the values of w_1, w_2, w, p_1, p_2 and $A_{\min}$ remain constant for all values of "$p_{\max}$", because the value of "p_1" does not reach the maximum pressure "$p_{\max}$". Case II: When the maximum pressure "$p_{\max}$" increases, y_0 and p_1 increase, w_1 and w decrease, w_2 and p_2 are equal.

Table 3 shows the following. Case I: There are no values, this is because it is restricted to w_1 and w_2 being equal, the value of w_2 needs a larger value, and therefore a radius greater than 20.00 m must be proposed. Case II: When the maximum pressure "$p_{\max}$" increases, y_0 and p_1 increase, w_1, w_2, w and $A_{\min}$ decrease, p_2 is equal.

Table 4 presents the following. Case I: When the axial load "P" decreases, w_1, w and $A_{\min}$ increase, p_1 decreases, w_2 and p_2 are equal. Case II: When the axial load "P" decreases, y_0 (absolute value), w_1, w and $A_{\min}$ increase, w_2, p_1 and p_2 are equal.

Table 5 shows the following. Case I: There are no values, this is because it is restricted to w_1 and w_2 being equal, the value of w_2 needs a larger value, and therefore a radius greater than 15.00 m must be proposed. Case II: When the axial load "P" decreases, y_0 (absolute value) decreases, w_1, w_2, w and $A_{\min}$ increase, p_1 and p_2 are equal.

Table 6 presents the following. Case I: When the resultant moment "M_R" increases, w_1, w and $A_{\min}$ increase, p_1 decreases, w_2 and p_2 are equal. Case II: When the resultant moment "M_R" increases, y_0 (absolute value) decreases, w_1, w and $A_{\min}$ increase, w_2, p_1 and p_2 are equal.

Table 7 shows the following. Case I: There are no values, this is because it is restricted to w_1 and w_2 being equal, the value of w_2 needs a larger value, and therefore a radius greater than 15.00 m must be proposed. Case II: When the resultant moment "M_R" increases, y_0 (absolute value) decreases, w_1, w_2, w and $A_{\min}$ increase, p_1 and p_2 are equal.

One way to check the new model is as follows.

1) Substituting $w_1 = 0$ into Equation (14) gives Equation (17) proposed by Soto-Garcia et al. [37].

2) Substituting $w_2 = 0$ into Equation (19) gives Equation (17) proposed by Soto-Garcia et al. [37].

3) Substituting $w_1 = 0$ into Equation (23) gives Equation (20) proposed by Soto-Garcia et al. [37].

4) Substituting $w_2 = 0$ into Equation (26) gives Equation (20) proposed by Soto-Garcia et al. [37].

Some comparisons are made with the results of other authors to show the advantages of the new model.

The practical example to consider the model proposed by Galvis and Smith-Pardo (G and S-P) [47] is shown below: A water tank of 24.3 m diameter by 36.6 m tall is perimetrically supported by a strip footing as shown in Figure 6. For a controlling load combination, overturning moment is $M_R = 300000$ kN-m and the corresponding gravity load at the base of the tank is $P = 28000$ kN. Determine the minimum width of the strip footing "w" to prevent the condition of vulnerable foundation for bearing capacity of the soil is "$p_{\max}$" equal to 500 kN/m^2, assuming $w_1 = w_2$.

The model proposed by Galvis and Smith-Pardo (G and S-P) [47] presents a minimum width of the strip footing of $w = 6.40$ m and $A_{\min} = 488.58$ m^2. While the model proposed in this work obtains the following results. The theoretical results are $y_0 = 4.34$ m, $w = 3.56$ m, $w_1 = 1.78$ m, $w_2 = 1.78$ m, $p_{\max} = 500$ kN/m^2 and $A_{\min} = 271.77$ m^2. The practical results are $y_0 = 4.32$ m, $w = 3.60$ m, $w_1 = 1.80$ m, $w_2 = 1.80$ m, $p_{\max} = 494.87$ kN/m^2 and $A_{\min} = 274.83$ m^2. Also, this problem is developed for $w_1 \neq w_2$ in new model, and the results are as the following. The theoretical values are $y_0 = 3.00$ m, $w = 2.96$ m, $w_1 = 1.96$ m, $w_2 = 1.00$ m, $p_{\max} = 500$ kN/m^2 and $A_{\min} = 234.54$ m^2. The practical

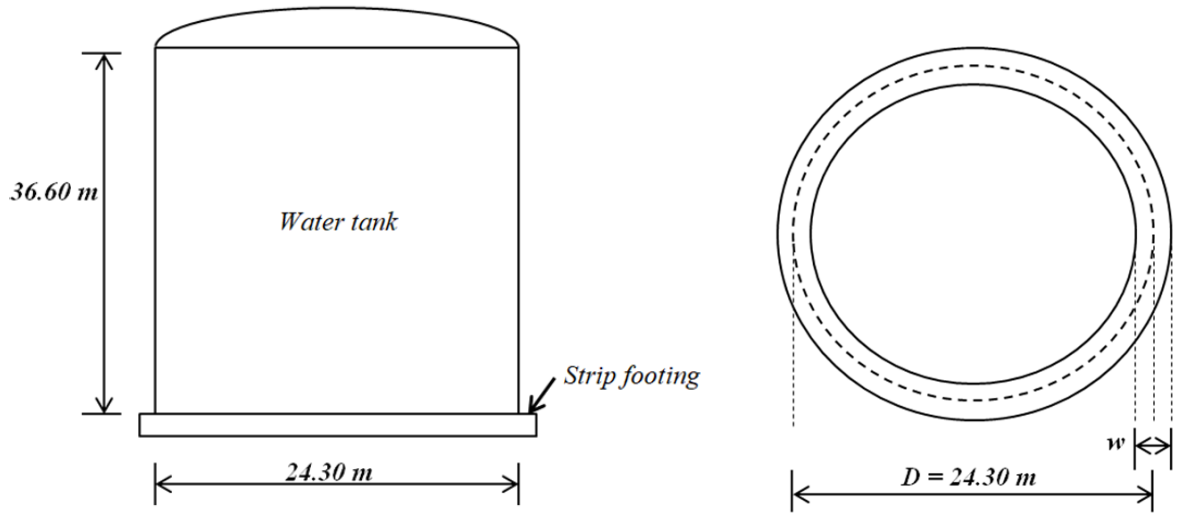

(a) Elevation view (b) Plan view

FIGURE 6. Water tank and strip footing

values are $y_0 = 2.91$ m, $w = 3.00$ m, $w_1 = 2.00$ m, $w_2 = 1.00$ m, $p_{\max} = 489.40$ kN/m^2 and $A_{\min} = 238.45$ m^2.

Therefore, the proposed model has a saving in the area of contact with the ground of 43.75% and the width of the annular strip footing of 43.75% with respect to the model proposed by Galvis and Smith-Pardo (G and S-P) [47] in practical value (assuming $w_1 = w_2$ for both models). Now, comparing the model proposed by (G and S-P) [47] in practical value (assuming $w_1 = w_2$) with the new model (assuming $w_1 \neq w_2$) there is a saving of 51.20% in the area of contact with the ground and the width of the annular strip footing of 53.12%. This is because the model proposed by Galvis and Smith-Pardo (G and S-P) [47] assumes a uniform soil pressure, and the proposed model assumes a linear soil pressure.

5. **Conclusions.** This paper presents a model to determine the optimal surface of a hollow circular footing or annular strip footing (the width and the position where pressure is zero, since the radius is subject to the conditions of the superstructure), assuming that the soil is elastic, the soil pressure distribution is linear and the surface in contact with the soil works partiality in compression.

The model consists of determining the width (w_1 and w_2) and the position where pressure is zero "y_0" of a hollow circular footing subjected to biaxial bending, taking account of the objective function that appears in Equation (28) and the constraint functions that appear in Table 1.

The contributions of this paper are as follows.

1.- Some works assume uniform soil pressure, and the external width of the foundation "w_1" is equal to the internal width of the foundation "w_2".

2.- The optimal area for case II is 0.0615 times that of case I at $p_{\max} = 100$ kN/m^2, 0.0440 times that of case I at $p_{\max} = 150$ kN/m^2, 0.0346 times that of case I at $p_{\max} = 200$ kN/m^2, 0.0286 times that of case I at $p_{\max} = 250$ kN/m^2, 0.0244 times that of case I at $p_{\max} = 300$ kN/m^2 (see Table 2).

3.- The optimal area for case II is 0.1070 times that of case I at $P = 28000$ kN, 0.0798 times that of case I at $P = 26000$ kN, 0.0615 times that of case I at $P = 24000$ kN, 0.0491 times that of case I at $P = 22000$ kN, 0.0414 times that of case I at $P = 20000$ kN (see Table 4).

4.- The optimal area for case II is 0.1245 times that of case I at $M_R = 240000$ kN-m, 0.0945 times that of case I at $M_R = 260000$ kN-m, 0.0778 times that of case I at $M_R = 280000$ kN-m, 0.0674 times that of case I at $M_R = 300000$ kN-m, 0.0608 times that of case I at $M_R = 320000$ kN-m (see Table 6).

5.- Tables 3, 5 and 7 do not have values for case I, this is because the radius is smaller than the interior width of the foundation ($R \leq w_2$).

6.- The proposed model has a saving in the ground contact area of 43.75% with respect to the model proposed by Galvis and Smith-Pardo (G and S-P) [47] in practical value.

The suggestions for the next research:

1.- Minimum cost design for hollow circular footings taking it into account that the surface in contact with the ground works partially in compression.

2.- Optimal surface in plan for hollow rectangular footings assuming that the contact surface with soil works partially under compression.

REFERENCES

[1] J. Khazaie and S. A. Amirshahkarami, Numerical analysis of interaction between earth and large foundations regarding size effect, *Journal of Applied Sciences*, vol.9, no.6, pp.1036-1045, 2009.

[2] M. Jahanandish, M. Veiskarami and A. Ghahramani, Effect of foundation size and roughness on the bearing capacity factor, $N\gamma$, by stress level-based ZEL method, *Arabian Journal for Science and Engineering*, vol.37, no.7, pp.1817-1831, 2012.

[3] G. A. Vyacheslavovich and B. L. Adolfovich, Influence of the form and size of the isolated foundations on the stress-strain state of the soil base, *Journal of Applied Engineering Science*, vol.14, no.1, pp.28-35, 2016.

[4] S. López-Chavarría, A. Luévanos-Rojas and M. Medina-Elizondo, A mathematical model for dimensioning of square isolated footings using optimization techniques: General case, *International Journal of Innovative Computing, Information and Control*, vol.13, no.1, pp.67-74, 2017.

[5] S. López-Chavarría, A. Luévanos-Rojas and M. Medina-Elizondo, Optimal dimensioning for the corner combined footings, *Advances in Computational Design*, vol.2, no.2, pp.169-183, 2017.

[6] A. Luévanos-Rojas, A mathematical model for dimensioning of footings square, *International Review of Civil Engineering*, vol.3, no.4, pp.346-350, 2012.

[7] A. Luévanos-Rojas, A mathematical model for the dimensioning of circular footings, *Far East Journal of Mathematical Sciences*, vol.71, no.2, pp.357-367, 2012.

[8] A. Luévanos-Rojas, A mathematical model for dimensioning of footings rectangular, *ICIC Express Letters, Part B: Applications*, vol.4, no.2, pp.269-274, 2013.

[9] W. L. Filho, R. C. Carvalho, A. L. Christoforo and F. A. R. Lahr, Dimensioning of isolated footing submitted to the under biaxial bending considering the low concrete consumption, *International Journal of Materials Engineering*, vol.7, no.1, pp.1-11, 2017.

[10] A. Luévanos-Rojas, A comparative study for dimensioning of footings with respect to the contact surface on soil, *International Journal of Innovative Computing, Information and Control*, vol.10, no.4, pp.1313-1326, 2014.

[11] A. Luévanos-Rojas, A new mathematical model for dimensioning of the boundary trapezoidal combined footings, *International Journal of Innovative Computing, Information and Control*, vol.11, no.4, pp.1269-1279, 2015.

[12] A. Luévanos-Rojas, A mathematical model for the dimensioning of combined footings of rectangular shape, *Revista Técnica de la Facultad de Ingeniería Universidad del Zulia*, vol.39, no.1, pp.3-9, 2016.

[13] A. Luévanos-Rojas, S. López-Chavarría and M. Medina-Elizondo, A new model for T-shaped combined footings Part I: Optimal dimensioning, *Geomechanics and Engineering*, vol.14, no.1, pp.51-60, 2018.

[14] G. Aguilera-Mancilla, A. Luévanos-Rojas, S. López-Chavarría and M. Medina-Elizondo, Modeling for the strap combined footings Part I: Optimal dimensioning, *Steel and Composite Structures*, vol.30, no.2, pp.97-108, 2019.

[15] M. A. Moreno-Hernandez, A. Luévanos-Rojas, S. López-Chavarría and M. Medina-Elizondo, Mathematical modeling for corner strap combined footings resting on the ground: Part 1, *Computación y Sistemas*, vol.26, no.3, pp.1259-1272, 2022.

[16] A. Luévanos-Rojas, J. G. Faudoa-Herrera, R. A. Andrade-Vallejo and M. A. Cano-Alvarez, Design of isolated footings of rectangular form using a new model, *International Journal of Innovative Computing, Information and Control*, vol.9, no.10, pp.4001-4022, 2013.

[17] S. López-Chavarría, A. Luévanos-Rojas and M. Medina-Elizondo, A new mathematical model for design of square isolated footings for general case, *International Journal of Innovative Computing, Information and Control*, vol.13, no.4, pp.1149-1168, 2017.

[18] A. Luévanos-Rojas, Design of isolated footings of circular form using a new model, *Structural Engineering and Mechanics*, vol.52, no.4, pp.767-786, 2014.

[19] A. Luévanos-Rojas, Minimum cost design for rectangular isolated footings taking into account that the column is located in any part of the footing, *Buildings*, vol.13, no.9, pp.1-16, 2023.

[20] A. Luévanos-Rojas, V. M. Moreno-Landeros, G. Santiago-Hurtado, F. J. Olguin-Coca, L. D. López-León and E. R. Diaz-Gurrola, Mathematical modeling for the optimal cost design of circular isolated footings with eccentric column, *Mathematics*, vol.12, no.5, pp.1-19, 2024.

[21] A. Luévanos-Rojas, Design of boundary combined footings of rectangular shape using a new model, *DYNA Colombia*, vol.81, no.188, pp.199-208, 2014.

[22] A. Luévanos-Rojas, S. López-Chavarría and M. Medina-Elizondo, A new model for T-shaped combined footings Part II: Mathematical model for design, *Geomechanics and Engineering*, vol.14, no.1, pp.61-69, 2018.

[23] J. A. Yáñez-Palafox, A. Luévanos-Rojas, S. López-Chavarría and M. Medina-Elizondo, Modeling for the strap combined footings Part II: Mathematical model for design, *Steel and Composite Structures*, vol.30, no.2, pp.109-121, 2019.

[24] M. L. Garcia-Graciano, A. Luévanos-Rojas, S. López-Chavarría and M. Medina-Elizondo, Mathematical modeling for corner strap combined footings resting on the ground: Part 2, *Computación y Sistemas*, vol.26, no.4, pp.1429-1443, 2022.

[25] A. Luévanos-Rojas, Optimization for trapezoidal combined footings: Optimal design, *Advances in Concrete Construction*, vol.16, no.1, pp.21-34, 2023.

[26] A. Luévanos-Rojas, G. Santiago-Hurtado, V. M. Moreno-Landeros, F. J. Olguin-Coca, L. D. López-León and E. R. Diaz-Gurrola, Mathematical modeling of the optimal cost for the design of strap combined footings, *Mathematics*, vol.12, no.2, pp.1-20, 2024.

[27] R. Irles-Más and F. Irles-Más, Alternativa analítica a la determinación de tensiones bajo zapatas rectangulares con flexión biaxial y despegue parcial (Explicit stresses under rectangular detached footings with biaxial bending), *Informes de la Construcción*, vol.44, no.419, pp.77-90, 1992.

[28] H. M. Algin, Stresses from linearly distributed pressures over rectangular areas, *International Journal for Numerical Analytical Methods in Geomechanics*, vol.24, no.8, pp.681-692, 2000.

[29] H. M. Algin, Practical formula for dimensioning a rectangular footing, *Engineering Structures*, vol.29, no.6, pp.1128-1134, 2007.

[30] G. Özmen, Determination of base stresses in rectangular footings under biaxial bending, *Teknik Dergi Digest*, vol.22, no.4, pp.1519-1535, 2011.

[31] J. Bellos and N. P. Bakas, High computational efficiency through generic analytical formulation for linear soil pressure distribution of rigid spread rectangular footings, *Proc. of the VII European Congress on Computational Methods in Applied Sciences and Engineering*, Crete Island, Greece, 2016.

[32] J. Bellos and N. P. Bakas, Complete analytical solution for linear soil pressure distribution under rigid rectangular spread footings, *International Journal of Geomechanics*, vol.17, no.7, https://doi.org/10.1061/(ASCE)GM.1943-5622.0000874, 2017.

[33] I. Aydogdu, New iterative method to calculate base stress of footings under biaxial bending, *International Journal of Engineering & Applied Sciences (IJEAS)*, vol.8, no.4, pp.40-48, 2016.

[34] K. Girgin, Simplified formulations for the determination of rotational spring constants in rigid spread footings resting on tensionless soil, *Journal of Civil Engineering and Management*, vol.23, no.4, pp.464-474, 2017.

[35] V. B. Vela-Moreno, A. Luévanos-Rojas, S. López-Chavarría, M. Medina-Elizondo, R. Sandoval-Rivas and C. Martínez-Aguilar, Optimal area for rectangular isolated footings considering that contact surface works partially to compression, *Structural Engineering and Mechanics*, vol.84, no.4, pp.561-573, 2022.

[36] V. M. Moreno-Landeros, A. Luévanos-Rojas, G. Santiago-Hurtado, L. D. López-León and E. R. Diaz-Gurrola, Optimal area for a rectangular isolated footing with an eccentric column and partial ground compression, *Applied Sciences*, vol.14, no.15, pp.1-16, 2024.

[37] S. Soto-Garcia, A. Luévanos-Rojas, J. D. Barquero-Cabrero, S. López-Chavarría, M. Medina-Elizondo, O. M. Farias-Montemayor and C. Martínez-Aguilar, A new model for the contact surface with soil of circular isolated footings considering that the contact surface works partially under compression, *International Journal of Innovative Computing, Information and Control*, vol.18, no.4, pp.1103-1116, 2022.

[38] I. Luévanos-Soto, A. Luévanos-Rojas, V. M. Moreno-Landeros and G. Santiago-Hurtado, Minimum area for circular isolated footings with eccentric column taking into account that the surface in contact with the ground works partially in compression, *Coupled Systems Mechanics*, vol.13, no.3, pp.201-217, 2024.

[39] A. Luévanos-Rojas, B. L. Estrada-Mendoza and M. Juárez-Ramirez, Comparative study for minimum areas in contact with the ground of rectangular and circular isolated footings working partially under compression, *Boletín Ciencias de la Tierra*, vol.55, no.1, pp.85-98, 2024.

[40] P. Montes-Paramo, A. Luévanos-Rojas, S. López-Chavarría, M. Medina-Elizondo and R. Sandoval-Rivas, Optimal area for rectangular combined footings assuming that contact surface with the soil works partially to compression, *Ingeniería Investigación y Tecnología*, vol.24, no.2, pp.1-15, 2023.

[41] A. Luévanos-Rojas, New model for complete design of rectangular isolated footings taking into account that the contact surface works partially in compression, *Revista ALCONPAT*, vol.10, no.3, pp.192-219, 2023.

[42] D. S. Kim-Sanchez, A. Luévanos-Rojas, J. D. Barquero-Cabrero, S. López-Chavarría, M. Medina-Elizondo and I. Luévanos-Soto, A new model for the complete design of circular isolated footings considering that the contact surface works partially under compression, *International Journal of Innovative Computing, Information and Control*, vol.18, no.6, pp.1769-1784, 2022.

[43] A. P. Singh-Rathor, J. K. Sharma and M. Madhira, An analytical study of annular raft on granular piles, *Studia Geotechnica et Mechanica*, vol.46, no.1, pp.21-44, 2024.

[44] B. S. Kim, O. Kwon, Y. H. Choi and J. K. Lee, Bearing capacity of annular foundations on rock mass with heterogeneous disturbance by finite element limit analysis, *Buildings*, vol.12, no.5, pp.1-11, 2022.

[45] K. S. Sankaran and M. S. Subrahmanyam, Analytical solution for annular ring-uniform loading contact pressure distribution to predict machine foundation response, *Soils and Foundations*, vol.13, no.3, pp.17-27, 1973.

[46] A. P. S. Rathor and J. K. Sharma, Engineering significance of annular raft foundations over solid raft foundations, *International Journal for Research in Applied Science & Engineering Technology*, vol.11, no.9, pp.930-934, 2023.

[47] F. A. Galvis and J. P. Smith-Pardo, Axial load biaxial moment interaction (PMM) diagrams for shallow foundations: Design aids, experimental verification, and examples, *Engineering Structures*, vol.213, 110582, 2020.

[48] S. K. Ahmad, V. Srinivasan and P. Ghosh, Analysis of annular footings and anchors lying on elastic soil medium using finite difference technique, *The 5th International Congress on Computational Mechanics and Simulation*, India, 2014.

[49] Y. Rana and A. Jamani, Comparative study of annular raft foundation & solid circular raft foundation for different diameter of water tank, *International Research Journal of Engineering and Technology*, vol.5, no.4, pp.3428-3436, 2018.

[50] R. Kumar and A. Rai, F.E.M analysis of annular mat foundation with & without annular beam, *International Research Journal of Engineering and Technology*, vol.10, no.10, pp.103-107, 2023.

[51] R. Manideep, A. V. R. Karthik and J. T. Chavda, Bearing capacity of strip, circular and ring footings on limited depth of soil, *Journal of GeoEngineering*, vol.18, no.4, pp.203-214, 2023.

Author Biography

Eyran Roberto Diaz-Gurrola received his B.Sc. degree in Industrial Engineering (2003), from the Instituto Tecnológico de Durango, Master in Senior Management (2010) from the Universidad Autónoma de Querétaro and the degree of Doctor in Senior Management (2015) from the Universidad Autónoma de Querétaro. He is professor and researcher of the Facultad de Contaduría y Administración, Torreón campus of the Universidad Autónoma de Coahuila. He is member of the National System of Researchers of Mexico (Candidate from 2022-2025). His research interests are mathematical models applied to engineering and administration.

Arnulfo Luévanos-Rojas received his B.Sc. degree in Civil Engineering (1981), Master in Science with Specialization in Structures (1983), Master in Science with Specialization in Planning and Construction of Works (2000), Master in Administration (2004), and Doctor in Engineering with Specialization in Planning Systems and Construction (2009). He was professor and researcher of the Facultad de Ingeniería, Ciencias y Arquitectura, Gomez Palacio Campus of the Universidad Juarez del Estado de Durango from 2006 to 2015, and of the Facultad de Contaduría y Administración, Torreón campus of the Universidad Autónoma de Coahuila since 2015 to date. He has published more than 137 papers in journals indexed in the Web of Science. His research interests are mathematical models applied to engineering and administration. He is member of the National System of Researchers of Mexico (Level I from 2016-2022 and Level II from 2023-2027). He is an Honorary State Researcher for the State of Coahuila, Mexico. He has received several distinctions: Distinguished Professor by ULSA (Universidad La Salle Laguna) 2002, 2007, 2010; Researcher of the year 2023 by UAC (Universidad Autónoma de Coahuila); Best scientific article of the year 2023 by UAC (Universidad Autónoma de Coahuila); He has been included in the "2023 World's Top 2% Scientists List" by Stanford University.

Gloria Josefina Montiel-Sánchez received her B.Sc. degree in Industrial Engineering (2000), from the Instituto Tecnológico de Durango. She is professor and researcher of the Centro de Estudios Tecnológicos Industriales y de Servicios No. 59, Torreón campus, Coahuila, México. Her research interests are mathematical models applied to engineering and administration.

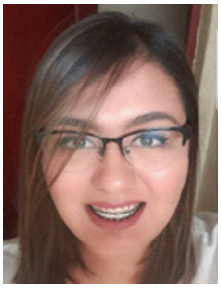

Carmela Martínez-Aguilar received the Master's degree in Administration and Senior Management (2012) and the degree of Doctor in Administration and Senior Management (2022) from the Facultad de Contaduría y Administración of the Universidad Autónoma de Coahuila. She is professor and researcher of the Facultad de Contaduría y Administración, Torreón campus of the Universidad Autónoma de Coahuila. Her research interests are mathematical models applied to administration.